

# **Understanding Vertical Land Motion in Eastern Indonesia and Its Implications to Regional Sea Level Rise**

**Maritsa Faridatun NISA, Paul DENYS, Chien Zheng YONG, Robert ODOLINSKI**  
**(New Zealand)**

**Key words:** vertical land motion; sea level rise; tectonic setting; satellite altimetry; tide gauges.

## **SUMMARY**

This study investigates the relationship between vertical land motion (VLM) and sea level rise (SLR) in eastern Indonesia, focusing on regions such as Sulawesi, North Maluku, Banda Sea, Nusa Tenggara, and Papua. The assessment of VLM has been undertaken using Global Navigation Satellite System (GNSS) data spanning up to 13 years that shows moderate rates of subsidence across these areas, largely driven by tectonic-induced motion. However, satellite altimetry and tide gauges observations reveal a significant SLR in eastern Indonesia, with rates exceeding global averages. The combination of land subsidence and acceleration of SLR poses serious risk to coastal communities, increasing vulnerability to flooding and shoreline erosion. This study emphasizes the necessity of incorporating VLM into disaster management strategies, highlighting the importance of continuous monitoring due to the region's active tectonic environment. The findings call for decision-making based on the inclusion of evidence from both land subsidence and SLR to ensure effective planning for future coastal resilience.

# Understanding Vertical Land Motion in Eastern Indonesia and Its Implications to Regional Sea Level Rise

Maritsa Faridatun NISA, Paul DENYS, Chien Zheng YONG, Robert ODOLINSKI  
(New Zealand)

## 1. INTRODUCTION

Vertical Land Motion (VLM) is the movement of the Earth's surface either upwards (uplift) or downwards (subsidence) and can be driven by several factors. For example, tectonic activity, such as fault movements and earthquakes, can cause significant shifts in land elevation. In coastal areas, the interaction of VLM with rising sea level rise (SLR) can exacerbate the vulnerability of these regions to erosion, saltwater erosion, and flooding. This is particularly relevant for Southeast Asia, where the combination of active tectonic processes and rising sea levels complicates the assessment of coastal risk.

Eastern Indonesia, characterized by its complex tectonic setting, comprising multiple active fault lines and volcanic activity, experiences spatially varying rates of VLM. This dynamic interplay between tectonic processes and VLM is especially important as it can significantly alter local sea level trends, complicating assessments of coastal vulnerability. These dynamics, however, have been underexplored in the context of SLR projections, which typically overlook the contributions of VLM. Despite some studies in specific regions like Palu Regency, Central Sulawesi, where geological and geodetic data have been used to assess land deformation following the 2018 Palu earthquake (Konagai et al., 2022; Song et al., 2019; Supendi et al., 2020) or in another localized region such as North Sulawesi, South Sulawesi, and West Nusa Tenggara (Handriyansyah, 2024; Pasaribu et al., 2021; Pasla et al., 2022) the integration of VLM and SLR assessments remains limited.

This paper aims to examine the VLM rates in the eastern part of Indonesia and their implications for SLR. Utilizing Global Navigation Satellite Systems (GNSS) data, this study investigates the land subsidence rates in the region which further can be compared with SLR trends. Preliminary findings suggest that most VLM rates indicate subsidence, which will have a worsening impact on coastal communities due to increasing sea level trends recorded from satellite altimetry and tide gauge observations. Ultimately, the findings of this study underscore the urgent need for further research in this underexplored area, providing critical insights for stakeholders and decision-makers navigating the complexities of coastal resilience.

## 2. LITERATURE REVIEW

In regions like Indonesia, which is located on the “Pacific Ring of Fire”, tectonic movements have a substantial impact on VLM (Fenoglio-Marc et al., 2012; Nandika et al., 2020). Sediment compaction is another major contributor, particularly in coastal deltas areas where the weight of accumulated sediments causes land to compress and therefore sink over time (Syvitski et al.,

2009). Human-induced activities such as groundwater extraction, mining, and urban development, can accelerate subsidence in many coastal regions. Groundwater withdrawal, in particular, causes land to sink as the underlying aquifers deplete. This is a well-documented phenomenon in cities like Jakarta, Kelantan, and Izmir (Abidin et al., 2011; Yalvaç et al., 2023; Yong et al., 2019). These factors can occur concurrently, making VLM a complex but critical variable in assessing coastal vulnerability to SLR.

Recent advancements in technology, particularly the use of GNSS in multi-constellation setups, have significantly improved the ability to measure VLM with high precision. Optimizing GNSS for VLM in sparsely observed areas using GPS/GNSS imaging can still provide bias correction due to network distribution (Hammond et al., 2016, 2021). Klos et al. (2019) introduced a VLM model that enhances estimates of sea level rates derived from tide gauge records influenced by seismic activity, allowing researchers to account for tectonic subsidence in their assessments. Furthermore, techniques such as Interferometric Synthetic Aperture Radar (InSAR) have been utilized to monitor land deformation across extensive areas, providing valuable insights into both natural and anthropogenic land motion (Huang & Yu, 2023; Yalvaç et al., 2023). These advancements in positioning methodology are crucial for improving the accuracy of land motion estimations, thereby enhancing our overall understanding of its interplay with SLR.

Localised sea level trends are highly correlated with VLM, complicating the assessment of SLR. Relative SLR (RSLR) rates in the region affected by VLM are up to four times higher than the global average, such as in Pacific Island countries, exacerbating flood risks and complicating SLR estimates (Hamlington et al., 2016; Nicholls et al., 2021). Klos et al. (2019) demonstrated that incorporating VLM models in the Western North Pacific can improve sea level rate estimates derived from tide gauge records influenced by earthquakes. Ignoring VLM and displacement due to tectonic movement could result in incorrect assessments of sea level trends from tide gauges of up to 10 mm/year. Similarly, Harvey et al. (2021) noted that VLM, alongside ocean mass changes and steric effects, largely explains RSLR along the US coast. It is crucial to account for VLM towards SLR in areas affected by land ice loss, glacial isostatic adjustment, land degradation due to human activities, and high tectonic activity (Denys et al., 2020). Neglecting VLM in sea level assessments can lead to serious underestimations of flood risks and erosion susceptibility.

In eastern Indonesia, the relationship between VLM and SLR is further complicated by the complex interplay of tectonic forces (Baillie et al., 2004; Morrice et al., 1983), and less due to local hydrology and human activities. Integrating VLM data into coastal management strategies is crucial to develop effective adaptation measures. Therefore, studying VLM and SLR in eastern Indonesia is essential for developing comprehensive strategies to protect and sustain these vulnerable coastal regions.

### **3. METHODOLOGY**

#### **3.1. Overview of Study Area**

Eastern Indonesia is situated within a multifaceted tectonic zone, which has been shaped by the Neogene collision and interplay of several plates: the Australian and Eurasian (Sundaland)

plates, the Caroline and Philippine Sea oceanic plates, and the Pacific Plate. The area is often compared to a massive jigsaw puzzle, composed of a network of small ocean basins divided by fragments or slivers of occasionally thickened continental crust, which appear to be ultimately converging to form a single intricate terrane (Figure 1). The region's active tectonics have been acknowledged for a long time and are distinctly manifested in its physical features, volcanic activity, and seismic events (Baillie et al., 2004). Numerous basins in the eastern part have evolved from the initial phases of arc-continent collision. A portion of these basins, including the Bay of Tomori (Figure 4) in eastern Sulawesi, have demonstrated potential for hydrocarbon exploration (Katili, 1991).

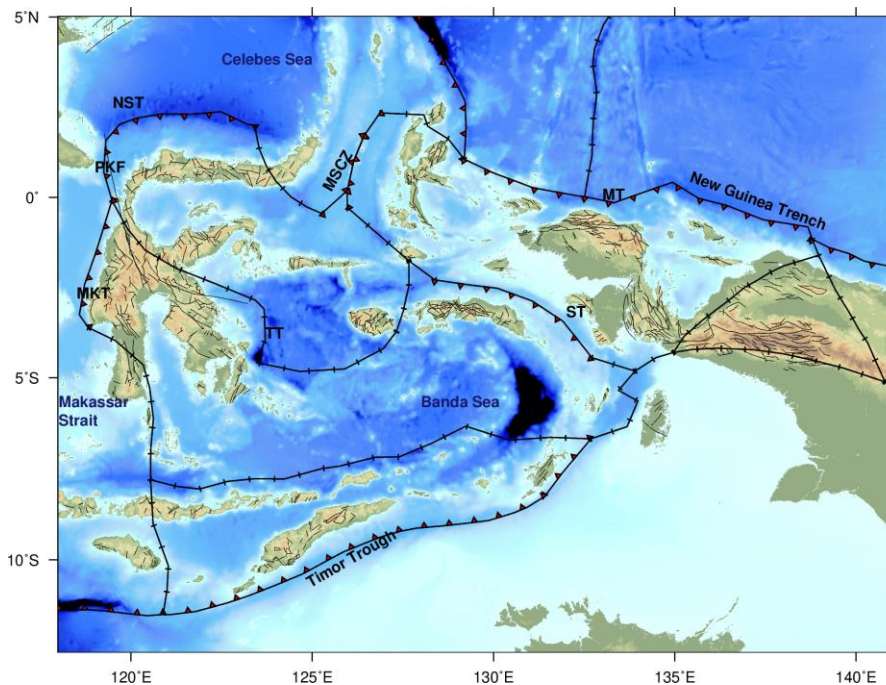


Figure 1. Tectonic map of eastern Indonesia. Lines with red triangles show the subduction zone and black lines with dash show fault and thrust lines, modified from Hutchings and Mooney (2021) and Bird (2003). Abbreviations: MKT = Makassar Thrust; PKF = Palu-Koro Fault; NST = Northern Sulawesi Trench; TT = Tolo Thrust; MSCZ = Molucca Sea Collision Zone; MT = Manokwari Trough; ST = Seram Trough. The bathymetry information is based on GEBCO.

Geographically, the eastern region of Indonesia covers Sulawesi, North Maluku, Banda Sea, Nusa Tenggara, and Papua. This area is marked by significant tectonic activity. Sulawesi, including North Sulawesi Sea, Maluku Sea, Banda Sea, and Makassar Strait is home to several notable fault lines, including the Palu-Koro Fault, which runs through the central part of the island and is known for its seismic activity (Hutchings & Mooney, 2021). Other than that, the regional tectonics is controlled by the North Sulawesi subduction zone, Maluku sea plate subduction along Sangihe, Matano fault, and the fault system around Banggai Islands that is a product of the collision of the Australian and Sunda Blocks, and the interaction between the

Philippine Sea and Caroline Plate. In addition to these fault lines, the Salawati Basin in Papua is an area of interest, characterized by sedimentary deposits that can influence local land subsidence due to compaction.

Nusa Tenggara, Banda, and North Maluku region are flanked by two earthquake sources: subduction from the south and back-arc thrust in the north. It is often referred to as the Sunda-Banda transition area, where tectonic forces shift from subduction to collision (Syuhada et al., 2016). Subduction forces dominate the western part of Nusa Tenggara, while collision forces influence the eastern part. This results in different seismicity patterns between the western and eastern regions. In North Maluku, frequent seismic activities are due to the interaction of multiple tectonic plates and the presence of the Sorong Fault Zone. The Banda Sea is seismically active due to the convergence of the Pacific, Indo-Australian, and Eurasian plates, with significant features like the Banda Arc and the Banda Detachment fault (Hamilton, 1973).

Papua is located on the western half of the New Guinea island. Tectonically, it is situated at the intersection of several major lithospheric plates: the Australian, Pacific, Philippine Sea, and Sunda plates. This region is further subdivided into microplates and deforming zones trapped in the collision of the Australian and Pacific Plates. In particular, the Bird's Head region of West Papua is dissected by several major strike-slip faults, including the Sorong, Ransiki, and Yapen faults (Gold et al., 2014). The Sorong Fault Zone (SFZ) is an active left-lateral fault system that has been active since the Late Miocene. The SFZ extends thousands of kilometres from Banggai in East Sulawesi to the Bird's Head region. The movement of SFZ involves rotation and translation that separates the Salawati Basin from the Bird's Head region with basement high as the boundary of the basin (Charlton, 1996; Riadini et al., 2012). Other local faults formed in this region and add complexity, such as the Seram fold-thrust belt, Tarera-Aiduna, Membramo fold-thrust belt, Aru through, and West fold-thrust belt (Badan Meteorologi Klimatologi dan Geofisika, 2021).

Coastal populations in eastern Indonesia, particularly in cities such as Makassar, Ambon, and Jayapura, face significant risks due to their proximity to the sea and the vulnerability of their regions to both natural disasters and climate change. These communities rely heavily on marine resources for their livelihoods, making them particularly susceptible to the impacts of rising sea levels and land subsidence. The interaction between VLM and SLR is thus a critical issue for local populations, necessitating comprehensive studies to inform effective environmental management and climate adaptation strategies.

### **3.2. Sites Distribution and Data Processing Technique**

This study utilized 34 GNSS observation sites in eastern Indonesia (Figure 2) as part of the Indonesian Continuously Operating Reference System (InaCORS) network that is operated by the Geospatial Agency of Indonesia (BIG). The GNSS data for this research is available from 2010 until 2023. Some stations with less than five years of data are still included in the processing and analysis to maintain data density and accommodate regions that do not have long-period GNSS stations. While the absence of extensive GNSS data can lead to unreliable estimates of annual trends, these shorter records still offer an insight into potential deformations that may have occurred at a site, and importantly, may identify high rates of VLM (both uplift

and subsidence). To represent International Terrestrial Reference Frame 2014 (ITRF2014), 56 International GNSS Service (IGS) sites were selected covering Asia, Australia, Antarctica, and Africa which lies on the Indian, Eurasia, Australia, Philippine Sea, Pacific, Antarctica, and Africa Plates.

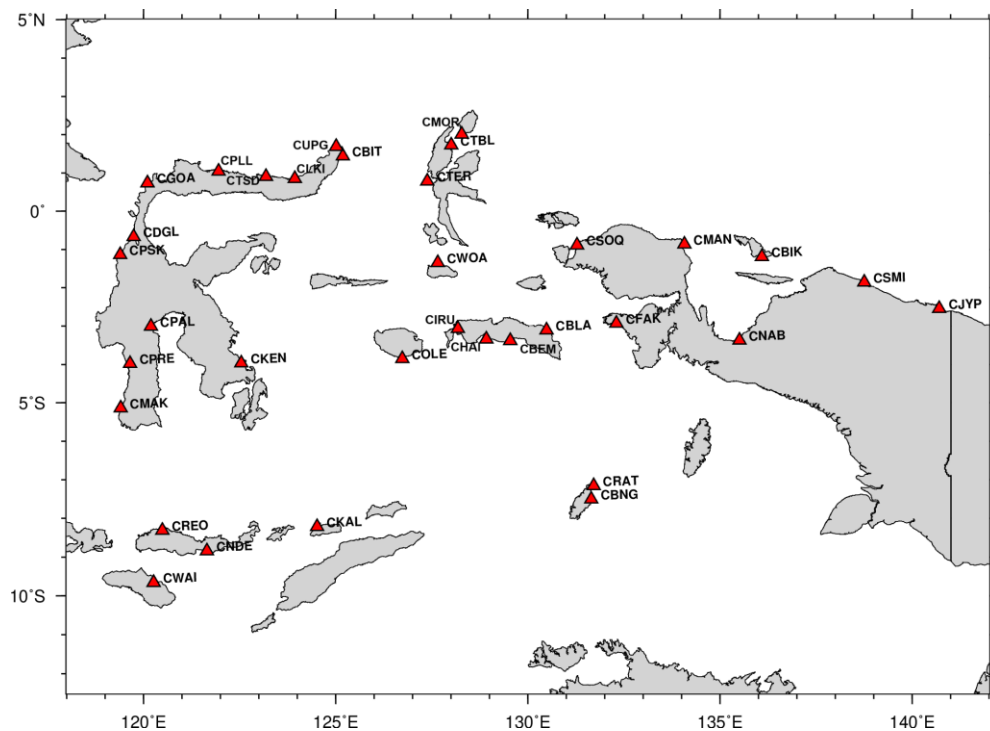


Figure 2. Distribution of InaCORS sites along the coast of east Indonesia.

The Bernese GNSS software (version 5.2) was utilized to process the GNSS observation data, including all Indonesian sites and the IGS network. Site velocities are determined from the position time series by processing the daily GNSS data. We utilize a double difference ionosphere-free combination in the processing scenario to eliminate most of the impact from the ionosphere on the baseline components. The parameter settings for data processing are based on the study by Yong et al. (2017). To maintain consistency with other data output, FES2014 is utilized in the processing for the loading tide, and ITRF2014 is also used as the station coordinate reference frame. **The processing of Indonesian and IGS sites was conducted using a clustering technique to improve correlation within a sparse GNSS network and eliminate white and flicker noise amplitude (Yong, 2019).**

This study focused on analysing the vertical component of GNSS observations. While the accuracy of the vertical component is affected by a number of systematic errors, such as, antenna phase centre variations, troposphere and ionospheric path delays, signal bending, atmospheric and hydrological loading, ice mass loss, and reference frame stability (Denys et al., 2020), GNSS observations can still provide long-term and continuous data to monitor any positional disturbances or movements at a GNSS site. The vertical trend determination using

GNSS data is also greatly influenced by the long-term consistency of the equipment hardware such as the antennas and receivers. Any hardware changes that occur throughout the time series must be recorded and taken into account in the processing (Denys et al., 2020). In the Bernese software, metadata preparation includes antenna/receiver changes as it is very important because it may significantly affect the GNSS vertical position and hence the vertical trend over time. **GNSS time series data in tectonically active regions are affected by various biases, such as seasonal variations, long-term rates, seismic-induced displacements and transient motions, which need to be parameterized when estimating velocity rates (Feng et al., 2015).**

Daily coordinates and their variances-covariances from Bernese processing are then used to determine the vertical velocity rates and uncertainty using a Matlab script (Plot Time Series, PTS) (Denys et al., 2016) using least square estimation. In this program all offsets, including both geometrical and geophysical, are modelled from the time series data to ensure that the vertical velocity rates are not affected by tectonic, seismic, or systematic errors (e.g. antenna changes). **Offsets in time series data are identified visually, which helps confirm their underlying causes, such as changes in the antenna or receiver, as well as co-seismic and post-seismic displacement or seasonal variations. When the epoch of an event is known, PTS estimates the magnitude of offsets by utilizing a Heaviside step function (Denys et al., 2016). This function, also called the unit step function, is particularly useful in modelling system that has sudden step or abrupt changes (Bracewell, 2000). Metadata records for the sites and earthquake catalogue provide information that can justify the offset that occurred at specific times. In cases where an earthquake is significant enough to trigger post-seismic relaxation (usually greater than 7 Mw), the script can effectively model this phenomenon using exponential, logarithmic, or power-law decay terms. The velocity from slow slip events can be parametrized using the error function, while seasonal changes are parameterized by including annual and semi-annual cyclic terms in the script (Denys et al., 2016). All offsets, both antenna/receiver changes and seismic-induced displacements, should be included in the time series model.**

#### **4. POST-2018 PALU EARTHQUAKE: LAND DEFORMATION IN THE SULAWESI REGION**

A destructive earthquake with a magnitude of 7.6 Mw occurred in 2018, with the epicentre located 70km from Palu City, Central Sulawesi Province (Figure 3). The earthquake was mainly caused by the movement of the Palu-Koro Fault as the major fault in the eastern part of Indonesia. At that time, there were not enough GNSS sites to adequately record the deformation caused by the earthquake; hence, the BIG established new GNSS sites in the region in 2019 in order to create a network of greater density. Following the main earthquake was a tsunami and liquefaction that caused economic losses of 13.8 trillion Indonesian rupiahs (~US \$980 million). In addition, it was found that the southern section of the Palu-Koro Fault exhibited higher seismicity at shallow depths compared to the northern section (Supendi et al., 2020).

Twelve InaCORS sites were established in this region, with the data span varying from 3 to 13 years (Table 1) (see Appendix A for a complete list of sites used in this study). The site's distribution and the vertical velocities are also shown in Figure 4. From GNSS observation, all

sites show subsidence at various rates. The biggest rates are concentrated in Central Sulawesi, where the Palu earthquake struck, and North Sulawesi, where complex tectonic interaction occurs. In Central Sulawesi, Ogoamas (CGOA), Donggala (CDGL), and Pasangkayu (CPSK) show subsidence at a rate of  $10.9 \pm 0.3$  mm/year,  $6.8 \pm 0.7$  mm/year, and  $5.6 \pm 0.3$  mm/year, respectively based on a short data span because the sites were installed after the 2018 earthquake. Even though the 2018 earthquake was triggered by a strike-slip mechanism around the Palu-Koro fault, a tsunami was produced afterwards due to the vertical movement of the sea floor near the overlying water mass. Strike-slip motion can also produce vertical displacement if the sea floor slope is steep ( $\sim 3$  m vertical offset), especially if it occurs in a fault zone (Hooper et al., 2013; Song et al., 2019).

Based on the significant earthquake and previous liquefaction, it is likely that the land subsidence in this area is linked to that event. Palu City, which is situated on young alluvial deposits, is located in an area with liquefiable sand layers, including the Palu-Koro rupture zone, which has thicker liquefiable sand layers, indicating a high potential for future liquefaction, especially in the event of a large earthquake (Tohari et al., 2023). Following the earthquake, the liquefied soil will remain unstable and soft, causing the deformation to persist for a prolonged time (Konagai et al., 2022). Clay soil has greater soil plasticity compared to silty or sandy soil, making it prone to permanent deformation even without experiencing cracking. Furthermore, lateral deformation causing horizontal movement of the soil also has the potential to occur after the liquefaction-causing earthquake (Kavazanjian et al., 2022).

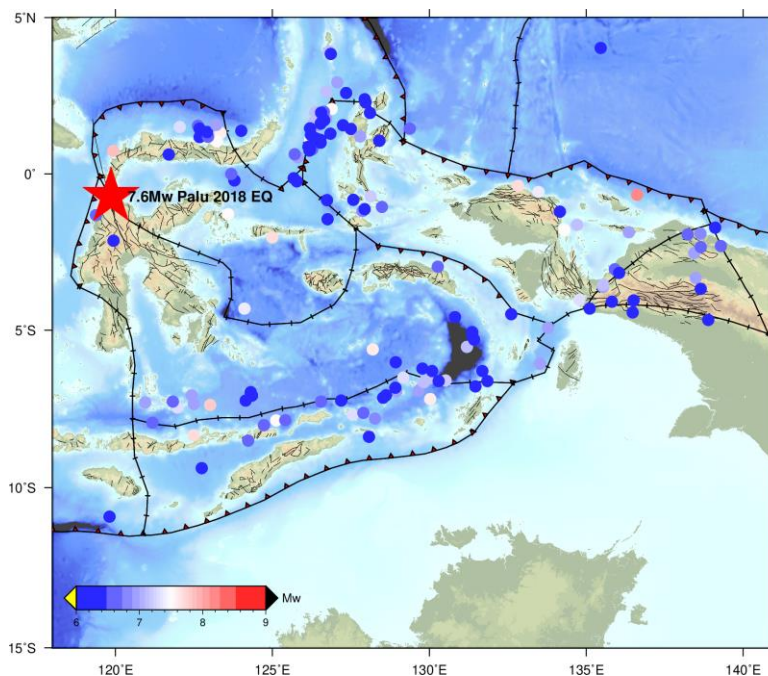


Figure 3. Earthquakes around Eastern Indonesia from 1985 until 2022 with moment magnitude above 6.0.

Table 1: Twelve sites distributed on Sulawesi Island with information on geodetic location, data availability, vertical velocity and its uncertainty ( $\sigma$ ).

Site	Lon. (E)	Lat. (N)	Data Span	Data Gaps (%)	Rate (mm/y)	$\sigma$ (mm/y)
CUPG	125.01°	1.69°	2019.96 - 2021.82	18.2	-9.14	0.82
CBIT	125.19°	1.44°	2010.0 - 2023.55	23.4	-5.32	2.43
CLKI	123.93°	0.85°	2019.94 - 2023.52	25.6	-2.20	0.37
CTSD	123.19°	0.91°	2019.93 - 2023.57	28.0	-1.68	0.38
CPLL	121.95°	1.04°	2019.96 - 2023.53	12.5	-3.07	0.33
CGOA	120.10°	0.74°	2019.94 - 2023.57	23.1	-10.91	0.33
CDGL	119.74°	-0.66°	2019.92 - 2021.74	2.9	-6.83	0.68
CPSK	119.39°	-1.14°	2019.93 - 2023.57	8.4	-5.57	0.32
CPAL	120.19°	-3.01°	2015.93 - 2023.57	5.9	0.12	0.13
CPRE	119.65°	-3.98°	2015.34 - 2021.93	6.2	-0.97	0.09
CMAK	119.41°	-5.13°	2010.00 - 2022.99	11	-2.01	0.07
CKEN	122.54°	-3.96°	2010.73 - 2021.99	10.2	-0.29	0.05

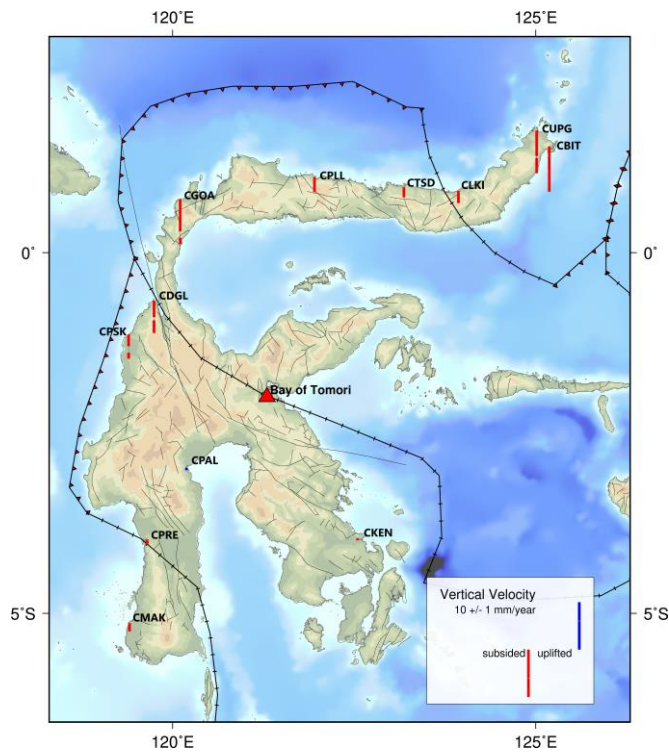


Figure 4: Vertical velocity in Sulawesi Island. Most sites exhibit subsidence and only one site shows minor uplift. Also shown is the location of the Bay of Tomori, where hydrocarbon potential has been found.

In North Sulawesi Province, there are five sites with subsidence rates ranging from 1.7 mm/year to 9.1 mm/year. Two sites, CBIT (Bitung) and CUPG (Likupang), located between Sangihe Trench and North Sulawesi Trench, show significant velocity rates of  $-5.3 \pm 2.4$  mm/year and  $-9.1 \pm 0.8$  mm/year respectively. Even though Northern Sulawesi is not as prone to liquefaction as the Central Sulawesi region, the collision between the Sangihe and Halmahera arcs may be the reason for high crustal activity in this region (Christy et al., 2018; Morrice et al., 1983). While the northern and central Sulawesi exhibit notable velocity rates, the remaining sites in Southern Sulawesi (CPAL, CPRE, CMAK, and CKEN) show minor vertical motion, with rates of less than 2 mm/year (Figure 4).

## 5. EARTHQUAKE-INDUCED VERTICAL DEFORMATION IN THE MALUKU AND NORTH MALUKU REGIONS

On 16 June 2021, a 6.0 Mw earthquake was recorded at a site in Tehoru (CBEM), Seram Island, Maluku. Research conducted by Daniarsyad et al. (2023) estimated that the earthquake was caused by a high-angle normal fault structure in the Tehoru subdistrict and Teluti Bay area. Geologically, Seram Island is located in the northern part of the Banda Arc and is categorized as a subduction structure developed by the Kawa shear zone, western Seram detachment zone, and high-angle normal faults. The earthquake resulted in a significant offset of  $\sim 40$  mm in the GNSS vertical component at the CBEM site (Figure 5). This displacement will cause inaccurate velocity trend estimation, so the offset must be parameterised in the time series data. The resulting trend estimate results in subsidence of  $4.3 \pm 0.6$  mm/y vertical velocity at the CBEM station (Figure 6, red line). Other sites located in Banda Arc and Maluku Island (COLE, CHAI, CIRU, and CBLA) show a subsidence pattern in various rates from 0 to 2.4 mm/year.

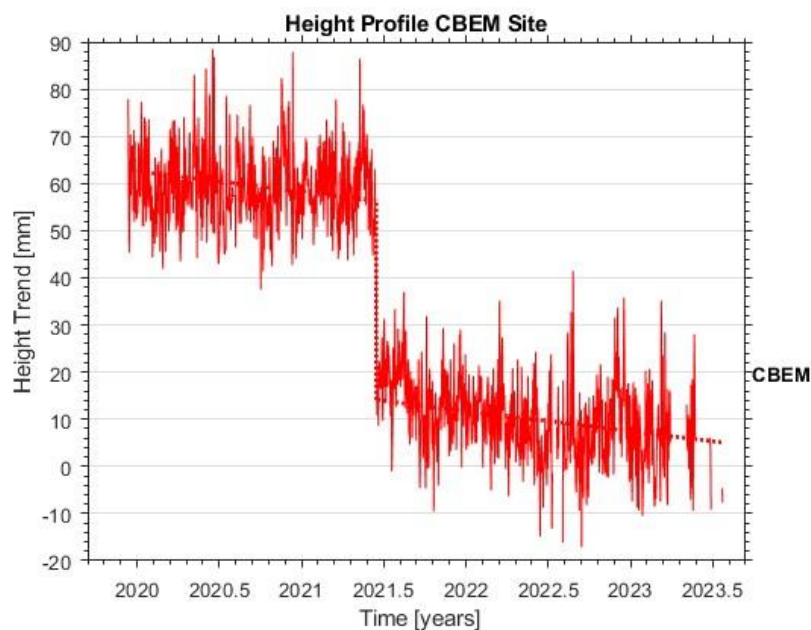


Figure 5. CBEM station in Seram Island recorded a 6.0 Mw earthquake with the epicentre located at the GNSS observation site. This event impacted the vertical position of the site and showed a co-seismic offset.

In North Maluku, four sites were involved in the study, but only two sites provided good-quality data. The CTBL and CTER sites, located in Tobelo and Ternate, recorded continuous observation data and showed subsidence at a rate of  $2.9 \pm 0.2$  mm/year and  $1.9 \pm 0.2$  mm/year, respectively. Some earthquakes with a magnitude of more than 7 Mw occurred during the data collection period, affecting the velocity estimation. Therefore, offsets should be taken into consideration. In the Flores Thrust Fault Zone, observation sites located in East Nusa Tenggara and Sumba (CWAI, CREO, CNDE) experience subsidence of approximately 1-3 mm/year, except for a site located in Kalabahi (CKAL) at Mutiara Bay, which experience uplift  $1.2 \pm 0.2$  mm/year (Figure 6).

## 6. VERTICAL VELOCITY IN PAPUA REGION

Seven stations were employed to monitor land movement of the coastal area in Papua region (Figure 7), two of which are situated in Manokwari (CMAN) and Nabire (CNAB). These two stations recorded an uplift of less than 3 mm/year. However, the remaining stations exhibited subsidence. The most significant subsidence rate was observed in Sorong (CSOQ), with a rate of  $7.1 \pm 0.3$  mm/year. It is strongly hypothesized that Sorong's substantial rate of subsidence is due to its location being influenced by the Sorong Fault Zone (SFZ) movements. The other stations, located in Sarmi (CSMI), Fak-fak (CFAK), Biak Numfor (CBIK), and Jayapura (CJYP), demonstrated varying subsidence rates of  $-0.3 \pm 0.1$  mm/year,  $2.4 \pm 0.1$  mm/year,  $-2.4 \pm 0.1$  mm/year, and  $-4.0 \pm 0.2$  mm/year, respectively.

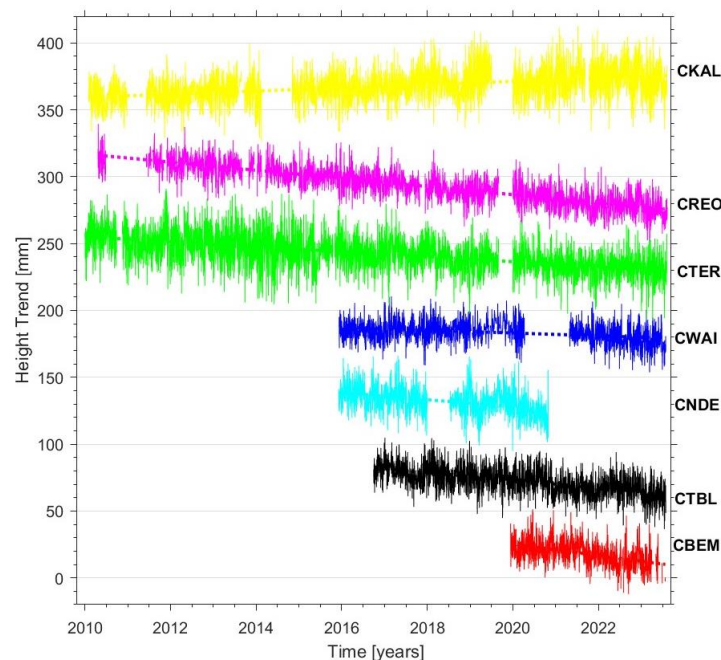


Figure 6. Height profiles of six stations located in North Maluku and East Nusa Tenggara. All sites exhibit subsidence, except CKAL in Kalabahi which show minor uplift.

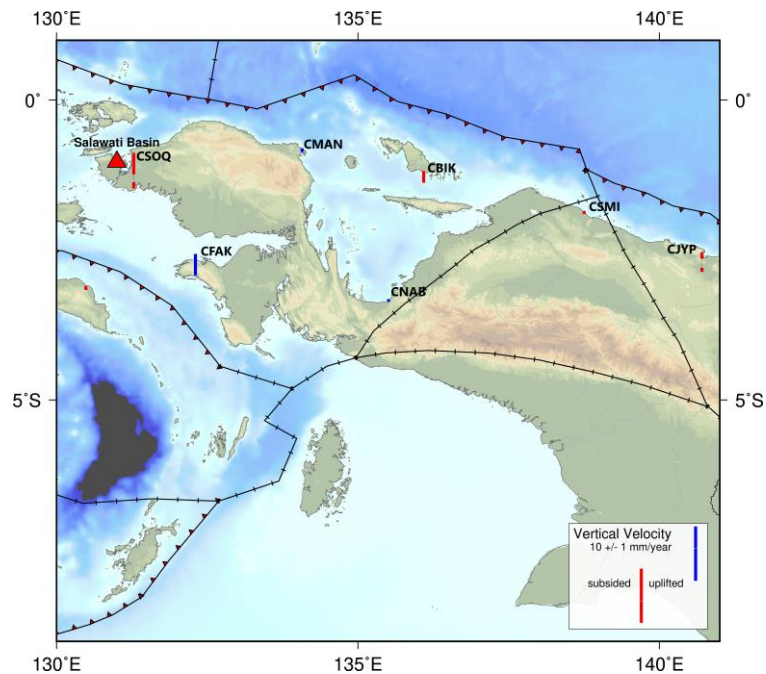


Figure 7. Vertical velocity from InaCORS sites around Papua/Irian Island. Most sites exhibit minor vertical displacement, except for two sites in Salawati Basin and Jayapura, which show subsidence.

## 7. THE IMPLICATION OF VLM AND SLR

The results of this study indicate that vertical velocity in eastern Indonesia across key regions such as Sulawesi, North Maluku, Banda Sea, Nusa Tenggara, and Papua have rates varying from 0 to 11 mm/year. The subsidence rates are generally significant when combined with the SLR trends derived from satellite altimetry data. Some studies have shown that SLR in the western Pacific, including the eastern Indonesian region, is among the highest globally, reaching up to 10 mm per year (Wang et al., 2015; World Meteorological Organization, 2023). From the tide gauge station, Bitung station located in North Sulawesi (co-located with CBIT station) also has a relative SLR trend with a rate of  $4.25 \pm 3.25$  mm/year based on 1986 to 2018 data from the Permanent Service for Mean Sea Level (PSMSL) archive. This substantial rise, coupled with ongoing subsidence, poses a serious threat to coastal areas, increasing the risks of flooding and shoreline erosion.

This combination of moderate land subsidence and significant SLR in eastern Indonesia amplifies the vulnerability of coastal areas to flooding, erosion, and other hazards. The discrepancy between VLM and sea level trends underscores the importance of incorporating VLM data into disaster management planning. Relying solely on SLR trends without considering subsidence could (significantly) underestimate the future impacts on coastal communities. For example, areas with moderate subsidence, when coupled with a rapidly rising sea level, could experience relative SLR far exceeding global averages, exacerbating coastal inundation risks.

## 8. CONCLUSION

This study underscores the importance of considering VLM in assessing the impacts of SLR in eastern Indonesia, where moderate subsidence combined with significant SLR exacerbates coastal risks. The findings highlight that relying solely on sea level trends without accounting for VLM underestimates the true hazards, as even moderate subsidence can significantly worsen coastal flooding and erosion (see Section 7). **The time series data indicate that most GNSS sites are either subsiding or uplifting at different rates, primarily due to tectonic activity. Some significant earthquakes have led to co-seismic displacements and post-seismic movements at various sites. Additionally, other sites are experiencing slow slip motions, attributed to their locations, which are continuously shifting over time.** Given the region's active tectonic environment, future VLM changes in coastal areas are likely, emphasizing the need for ongoing monitoring and adaptive coastal management. **In addition to gradual trends, the potential for sudden elevation changes requires the development of rapid response strategies to mitigate the impacts on coastal populations and infrastructure due to altered flooding scenarios.** Effective coastal disaster management strategies must integrate both VLM and SLR data to better protect vulnerable coastal communities from future risks.

## REFERENCES

- Abidin, H. Z., Andreas, H., Gumilar, I., Fukuda, Y., Pohan, Y. E., & Deguchi, T. (2011). Land subsidence of Jakarta (Indonesia) and its relation with urban development. *Natural Hazards*, 59(3), 1753–1771. <https://doi.org/10.1007/s11069-011-9866-9>
- Badan Meteorologi Klimatologi dan Geofisika. (2021). *Katalog Gempabumi Indonesia: Relokasi Hiposenter dan Implikasi Tektonik*.
- Baillie, P. W., Fraser, T. H., Hall, R., & Myers, K. (2004). Geological development of eastern Indonesia and the northern Australia collision zone: A review. *Proceedings of the Timor Sea Symposium*, 539–550. [http://topex.ucsd.edu/marine\\_grav/mar\\_grav.html](http://topex.ucsd.edu/marine_grav/mar_grav.html)
- Bird, P. (2003). An updated digital model of plate boundaries. *Geochemistry, Geophysics, Geosystems*, 4(3). <https://doi.org/10.1029/2001GC000252>
- Bracewell, R. (2000). The fourier transform and its applications (3rd edition). New York: McGraw-Hill, pp. 61-65.
- Charlton, T. R. (1996). Correlation of the Salawati and Tomori Basins, eastern Indonesia: A constraint on left-lateral displacements of the Sorong fault zone. *Geological Society Special Publication*, 106, 465–481. <https://doi.org/10.1144/GSL.SP.1996.106.01.29>
- Christy, K., Oktovian, T., Sompie, B. A., & Ticoh, J. H. (2018). Analisis Potensi Likuifaksi Tanah Berdasarkan Data Standart Penetration Test (SPT) Studi Kasus : Dermaga Blitung, Sulawesi Utara. *Jurnal Sipil Statik*, 6(7), 491–500.
- Daniarsyad, G., Priyobudi, P., Cahyaningrum, A. P., Wibisono, D. G., Sriyanto, S. P. D., Rosid, A., Pranata, B., Gunawan, I., Fatchurochman, I., & Daryono, D. (2023). Analysis on the Causative Fault of the 2021 Mw 6.0 Tehoru Earthquake in the South Coast of Seram Island: A Preliminary Result. *E3S Web of Conferences*, 447. <https://doi.org/10.1051/e3sconf/202344701020>
- Denys, P. H. (2023). *Plot Time Series (pts)* (23.07). School of Surveying, University of Otago.
- Denys, P. H., Beavan, R. J., Hannah, J., Pearson, C. F., Palmer, N., Denham, M., & Hreinsdottir, S. (2020). Sea Level Rise in New Zealand: The Effect of Vertical Land Motion on Century-Long Tide Gauge Records in a Tectonically Active Region. *Journal of Geophysical Research: Solid Earth*, 125(1). <https://doi.org/10.1029/2019JB018055>
- Denys, P., Pearson, C., Norris, R., & Denham, M. (2016). A geodetic study of Otago: results of the central Otago deformation network 2004–2014. *New Zealand Journal of Geology and Geophysics*, 59(1), 147–156. <https://doi.org/10.1080/00288306.2015.1134592>
- Feng, L., Hill, E. M., Banerjee, P., Hermawan, I., Tsang, L. L. H., Natawidjaja, D. H., Suwargadi, B. W., & Sieh, K. (2015). A unified GPS-based earthquake catalog for the Sumatran plate boundary between 2002 and 2013. *Journal of Geophysical Research: Solid Earth*, 120(5), 3566–3598. <https://doi.org/10.1002/2014JB011661>
- Fenoglio-Marc, L., Schöne, T., Illigner, J., Becker, M., Manurung, P., & Khafid. (2012). Sea Level Change and Vertical Motion from Satellite Altimetry, Tide Gauges and GPS in the Indonesian Region. *Marine Geodesy*, 35(SUPPL. 1), 137–150. <https://doi.org/10.1080/01490419.2012.718682>
- Gold, D., Hall, R., Burgess, P., & Boudagher-Fadel, M. (2014). *The Biak Basin and Its Setting in the Bird's Head Region of West Papua*.
- Hamilton, W. (1973). Tectonics of the Indonesian Region \*. In *Geol. Soc. Malaysia, Bulletin* (Vol. 6).
- Hamlington, B. D., Thompson, P., Hammond, W. C., Blewitt, G., & Ray, R. D. (2016). Assessing the impact of vertical land motion on twentieth century global mean sea level estimates. *Journal of Geophysical Research: Oceans*, 121(7), 4980–4993. <https://doi.org/10.1002/2016JC011747>
- Hammond, W. C., Blewitt, G., & Kreemer, C. (2016). GPS Imaging of vertical land motion in California and Nevada: Implications for Sierra Nevada uplift. *Journal of Geophysical Research: Solid Earth*, 121(10), 7681–7703. <https://doi.org/10.1002/2016JB013458>
- Hammond, W. C., Blewitt, G., Kreemer, C., & Nerem, R. S. (2021). GPS Imaging of Global Vertical Land Motion for Studies of Sea Level Rise. *Journal of Geophysical Research: Solid Earth*, 126(7). <https://doi.org/10.1029/2021JB022355>
- Handriyansyah, M. P. (2024). *Uji Akurasi Nilai Ketelitian Settlement Point untuk Mengetahui Penurunan Tanah Pada Bendungan Tipe Urugan (Studi Kasus: Kecamatan Praya Barat, Kabupaten Lombok Tengah, Provinsi Nusa Tenggara Barat)*. ITN Malang.
- Harvey, T. C., Hamlington, B. D., Frederikse, T., Nerem, R. S., Piecuch, C. G., Hammond, W. C., Blewitt, G., Thompson, P. R., Bekaert, D. P. S., Landerer, F. W., Reager, J. T., Kopp, R. E., Chandanpurkar, H., Fenty, I., Trossman, D., Walker, J. S., & Boening, C. (2021). Ocean mass, steric effects, and vertical land motion largely explain US coast relative sea level rise. *Communications Earth and Environment*, 2(1). <https://doi.org/10.1038/s43247-021-00300-w>

- Hooper, A., Pietrzak, J., Simons, W., Cui, H., Riva, R., Naeije, M., Terwisscha van Scheltinga, A., Schrama, E., Stelling, G., & Socquet, A. (2013). Importance of horizontal seafloor motion on tsunami height for the 2011 Mw=9.0 Tohoku-Oki earthquake. *Earth and Planetary Science Letters*, 361, 469–479. <https://doi.org/10.1016/j.epsl.2012.11.013>
- Huang, Z., & Yu, F. (2023). InSAR-derived surface deformation of Chaoshan Plain, China: Exploring the role of human activities in the evolution of coastal landscapes. *Geomorphology*, 426. <https://doi.org/10.1016/j.geomorph.2023.108606>
- Hutchings, S. J., & Mooney, W. D. (2021). The Seismicity of Indonesia and Tectonic Implications. *Geochemistry, Geophysics, Geosystems*, 22(9). <https://doi.org/10.1029/2021GC009812>
- Katili, J. A. (1991). Tectonic evolution of eastern Indonesia and its bearing on the occurrence of hydrocarbons. *Marine and Petroleum Geology*, 8(1), 70–83. [https://doi.org/10.1016/0264-8172\(91\)90046-4](https://doi.org/10.1016/0264-8172(91)90046-4)
- Kavazanjian, E., Andrade, J. E., Arulmoli, K. A., Atwater, B. F., Christian, J. T., Green, R., Kramer, S. L., Mejia, L., Mitchell, J. K., Rathje, E., Rice, J. R., Wang, Y., Magsino, S., & Gibbs, C. R. (2022). State of the Art and Practice in the Assessment of Earthquake-Induced Soil Liquefaction and Its Consequences. In *State of the Art and Practice in the Assessment of Earthquake-Induced Soil Liquefaction and Its Consequences*. National Academies Press. <https://doi.org/10.17226/23474>
- Klos, A., Kusche, J., Fenoglio-Marc, L., Bos, M. S., & Bogusz, J. (2019). Introducing a vertical land motion model for improving estimates of sea level rates derived from tide gauge records affected by earthquakes. *GPS Solutions*, 23(4). <https://doi.org/10.1007/s10291-019-0896-1>
- Konagai, K., Furuta, R., & Kiyota, T. (2022). Widespread ground deformation over the Palu Basin caused by the 2018 Sulawesi, Indonesia Earthquake. *JSCE Journal of Disaster FactSheets*.
- Morrice, M. G., Jezek, P. A., Gill, J. B., Whitford, D. J., & Monoarfa, M. (1983). An Introduction to the Sangihe Arc: Volcanism Accompanying Arc-Arc Collision in the Molucca Sea, Indonesia. *Journal of Volcanology and Geothermal Research*, 19, 135–165.
- Nandika, M. R., Susilo, S. B., & Siregar, V. (2020). Vertical Land Motion and Inundation Processes Based on the Integration of Remotely Sensed Data and IPCC AR5 Scenarios in Coastal Semarang, Indonesia. *International Journal of Remote Sensing and Earth Sciences (IJReSES)*, 16(2), 121. <https://doi.org/10.30536/j.ijreses.2019.v16.a3272>
- Nicholls, R. J., Lincke, D., Hinkel, J., Brown, S., Vafeidis, A. T., Meyssignac, B., Hanson, S. E., Merkens, J. L., & Fang, J. (2021). A global analysis of subsidence, relative sea-level change and coastal flood exposure. *Nature Climate Change*, 11(4), 338–342. <https://doi.org/10.1038/s41558-021-00993-z>
- Pasaribu, R. A., Budi, P. S., Hakim, M. A. G. A., Aditama, F. A., & Ayuningtyas, N. H. (2021). Coastal Inundation Model in the Coastal Area of Palopo City, South Sulawesi Province. *Journal of Applied Geospatial Information*, 5(1).
- Pasla, F. R., Sompie, O. B. A., & Rondonuwu, S. G. (2022). Kajian Gerakan Tanah dan Penanggulangannya Pada Ruas Jalan Worotican - Poopo - Sinisir Propinsi Sulawesi Utara. *Jurnal Ilmiah Media Engineering*, 12(1), 81–98.
- Riadini, P., Sapiie, B., & Surya Nugraha, A. M. (2012). *The Sorong Fault Zone Kinematics: Implication for Structural Evolution on Salawati Basin, Seram and Misool, West Papua, Indonesia*.
- Song, X., Zhang, Y., Shan, X., Liu, Y., Gong, W., & Qu, C. (2019). Geodetic Observations of the 2018 Mw 7.5 Sulawesi Earthquake and Its Implications for the Kinematics of the Palu Fault. *Geophysical Research Letters*, 46(8), 4212–4220. <https://doi.org/10.1029/2019GL082045>
- Supendi, P., Nugraha, A. D., Widiyantoro, S., Pesicck, J. D., Thurber, C. H., Abdullah, C. I., Daryono, D., Wiyono, S. H., Shiddiqi, H. A., & Rosalia, S. (2020). Relocated aftershocks and background seismicity in eastern Indonesia shed light on the 2018 Lombok and Palu earthquake sequences. *Geophysical Journal International*, 221(3), 1845–1855. <https://doi.org/10.1093/gji/ggaa118>
- Syhada, S., Hananto, N. D., Abdullah, C. I., Puspito, N. T., Anggono, T., & Yudistira, T. (2016). Crustal Structure Along Sunda-Banda Arc Transition Zone from Teleseismic Receiver Functions. *Acta Geophysica*, 64(6), 2020–2050. <https://doi.org/10.1515/acgeo-2015-0098>
- Syvitski, J. P. M., Kettner, A. J., Overeem, I., Hutton, E. W. H., Hannon, M. T., Brakenridge, G. R., Day, J., Vörösmarty, C., Saito, Y., Giosan, L., & Nicholls, R. J. (2009). Sinking deltas due to human activities. *Nature Geoscience*, 2(10), 681–686. <https://doi.org/10.1038/ngeo629>
- Tohari, A., Soebowo, E., Wibawa, S., Hermawan, K., & Saputra, O. F. (2023). Liquefaction potential analysis for Palu City based on CPT method. *IOP Conference Series: Earth and Environmental Science*, 1173(1). <https://doi.org/10.1088/1755-1315/1173/1/012030>
- Wang, T. Y., Du, Y., Zhuang, W., & Wang, J. B. (2015). Connection of sea level variability between the tropical western Pacific and the southern Indian Ocean during recent two decades. *Science China Earth Sciences*, 58(8), 1387–1396. <https://doi.org/10.1007/s11430-014-5048-4>
- World Meteorological Organization. (2023). *State of the Climate in the South-West Pacific 2023*.

---

Understanding Vertical Land Motion in Eastern Indonesia and Its Implications to Regional Sea Level Rise (13033)  
Maritsa Faridatun Nisa, Paul Denys, Chien Zheng Yong and Robert Odolinski (New Zealand)

FIG Working Week 2025

Collaboration, Innovation and Resilience: Championing a Digital Generation

Brisbane, Australia, 6–10 April 2025

- Yalvaç, S., Alemdağ, S., Zeybek, H. İ., & Yalvaç, M. (2023). Excessive groundwater withdrawal and resultant land subsidence in the Küçük Menderes River Basin, Turkey as estimated from InSAR-SBAS and GNSS measurements. *Advances in Space Research*, 72(10), 4282–4297. <https://doi.org/10.1016/j.asr.2023.08.001>
- Yong, C. Z. (2019). Tectonic geodesy: an analysis of the crustal deformation of the western Sundaland plate from nearly two decades of continuous GPS measurements, *Doctoral dissertation*, University of Otago.
- Yong, C. Z., Denys, P. H., & Pearson, C. F. (2017). Present-day kinematics of the Sundaland plate. *Journal of Applied Geodesy*, 11(3), 169–177.
- Yong, C. Z., Denys, P. H., & Pearson, C. F. (2019). Groundwater extraction-induced land subsidence: a geodetic strain rate study in Kelantan, Malaysia. In *Journal of Spatial Science* (Vol. 64, Issue 2, pp. 275–286). Mapping Sciences Institute Australia. <https://doi.org/10.1080/14498596.2018.1429329>

## BIOGRAPHICAL NOTES

### CONTACTS

Maritsa Nisa, M.Eng.  
School of Surveying, University of Otago, New Zealand  
310 Castle Street  
Dunedin  
NEW ZEALAND  
Tel. +64223021791  
Email: [nisma474@student.otago.ac.nz](mailto:nisma474@student.otago.ac.nz)

Maritsa is a PhD candidate at the School of Surveying, University of Otago, New Zealand. Her research interests focus on geodesy, including positioning and vertical land motion using GNSS, and satellite altimetry related to sea level rise, hydrography, and climate change.

APPENDIX A.

List of GNSS sites for this research with the location, time span, vertical velocity and uncertainty information.

Site	Lon. (E)	Lat. (N)	Data Span	Data Gaps (%)	Rate (mm/y)	$\sigma$ (mm/y)
CUPG	125.01°	1.69°	2019.96 - 2021.82	18.2	-9.14	0.82
CBIT	125.19°	1.44°	2010.00 - 2023.55	23.4	-5.32	2.43
CLKI	123.93°	0.85°	2019.94 - 2023.52	25.6	-2.20	0.37
CTSD	123.19°	0.91°	2019.93 - 2023.57	28.0	-1.68	0.38
CPLL	121.95°	1.04°	2019.96 - 2023.53	12.5	-3.07	0.33
CGOA	120.10°	0.74°	2019.94 - 2023.57	23.1	-10.91	0.33
CDGL	119.74°	-0.66°	2019.92 - 2021.74	2.9	-6.83	0.68
CPSK	119.39°	-1.14°	2019.93 - 2023.57	8.4	-5.57	0.32
CPAL	120.19°	-3.01°	2015.93 - 2023.57	5.9	0.12	0.13
CPRE	119.65°	-3.98°	2015.34 - 2021.93	6.2	-0.97	0.09
CMAK	119.41°	-5.13°	2010.00 - 2022.99	11.0	-2.01	0.07
CKEN	122.54°	-3.96°	2010.73 - 2021.99	10.2	-0.29	0.05
CREO	120.49°	-8.31°	2010.30 - 2023.61	16.6	-3.04	0.08
CNDE	121.65°	-8.84°	2015.93 - 2020.83	11.8	-2.68	0.16
CWAI	120.26°	-9.65°	2015.94 - 2023.57	22.8	-1.06	0.08
CKAL	124.52°	-8.21°	2010.09 - 2023.60	15.0	1.20	0.18
CMOR	128.28°	2.02°	2019.93 - 2023.41	76.7	-3.63	0.46
CTBL	128.01°	1.73°	2016.75 - 2023.57	1.2	-2.86	0.23
CTER	127.38°	0.79°	2010.00 - 2023.60	6.1	-1.87	0.17
CWOA	127.66°	-1.34°	2019.95 - 2023.38	83.1	-2.88	0.60
COLE	126.73°	-3.85°	2019.96 - 2023.57	54.6	-0.59	0.52
CIRU	128.18°	-3.07°	2019.98 - 2023.57	5.1	-2.35	0.34
CHAI	128.92°	-3.34°	2019.95 - 2023.57	18.0	-0.03	0.30
CBEM	129.54°	-3.38°	2019.95 - 2023.56	10.0	-4.29	0.59
CBLA	130.49°	-3.10°	2016.73 - 2023.57	1.4	-0.15	0.33
CRAT	131.71°	-7.15°	2019.94 - 2022.49	25.4	-5.10	0.40
CBNG	131.65°	-7.50°	2020.00 - 2023.56	54.2	-9.97	4.05
CSOQ	131.28°	-0.88°	2017.20 - 2023.57	22.7	-7.14	0.30
CMAN	134.07°	-0.86°	2010.00 - 2023.59	13.6	0.58	0.05
CBIK	136.09°	-1.19°	2010.00 - 2023.57	13.4	-2.42	0.10
CNAB	135.51°	-3.37°	2010.00 - 2023.59	7.4	0.52	0.04
CSMI	138.75°	-1.85°	2016.71 - 2023.57	15.2	-0.34	0.14
CJYP	140.70°	-2.54°	2016.79 - 2023.57	11.8	-4.00	0.18
CFAK	132.30°	-2.92°	2010.81 - 2023.59	41.0	2.99	0.78